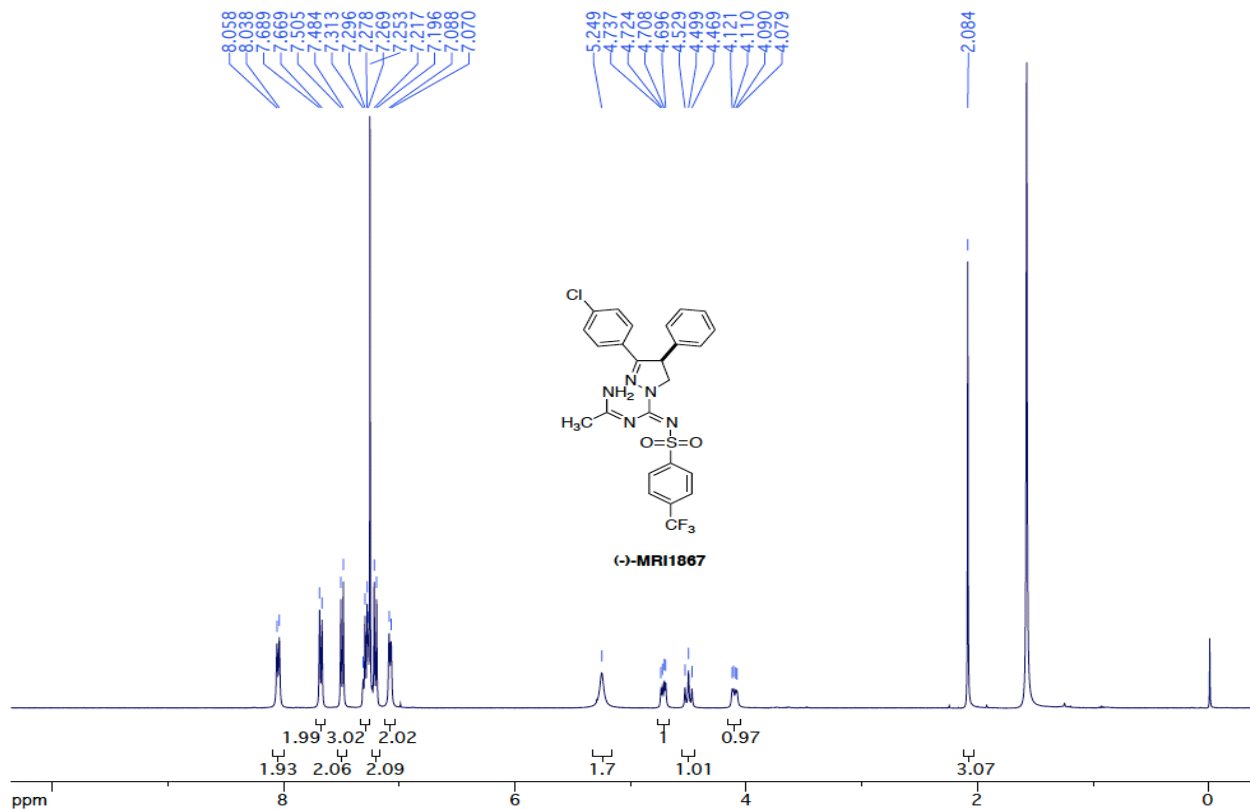


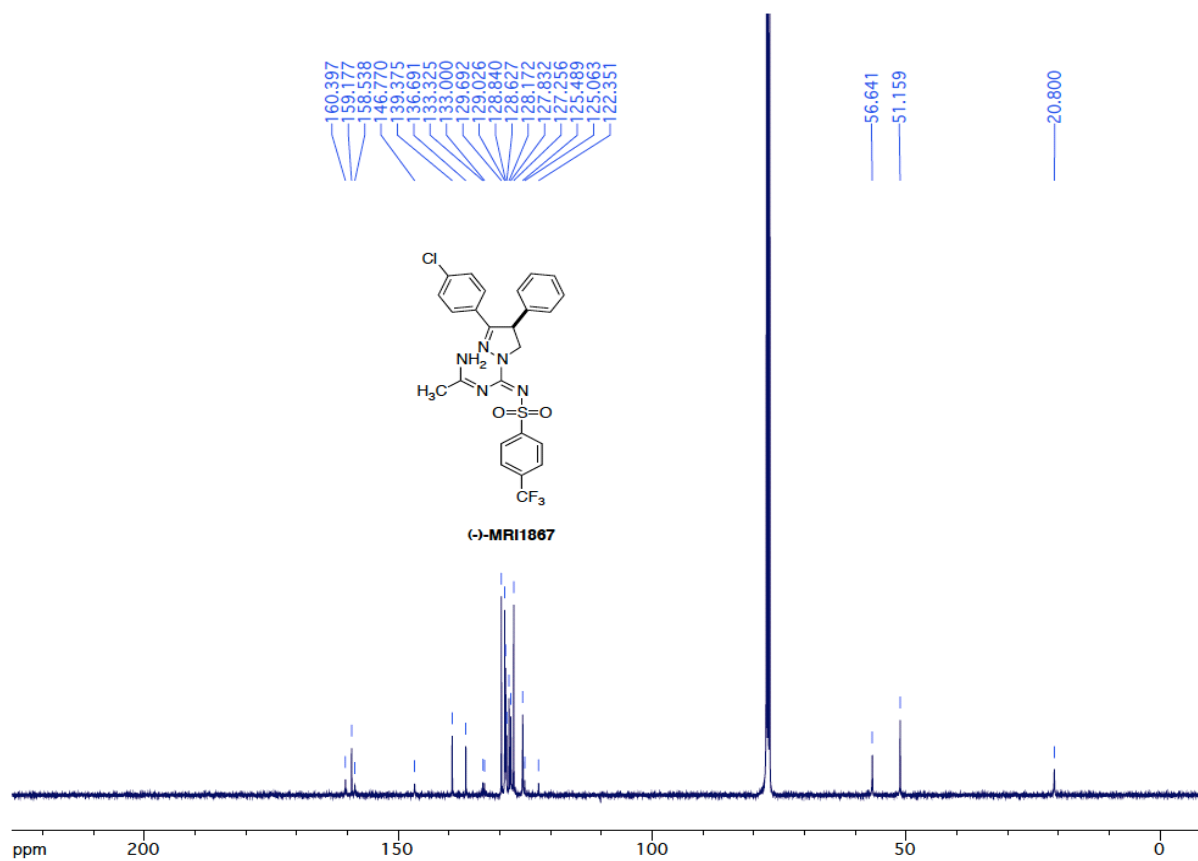
## Supplemental Figures and Tables

### **Hybrid inhibitor of peripheral cannabinoid 1 receptors and inducible nitric oxide synthase for the treatment of liver fibrosis**

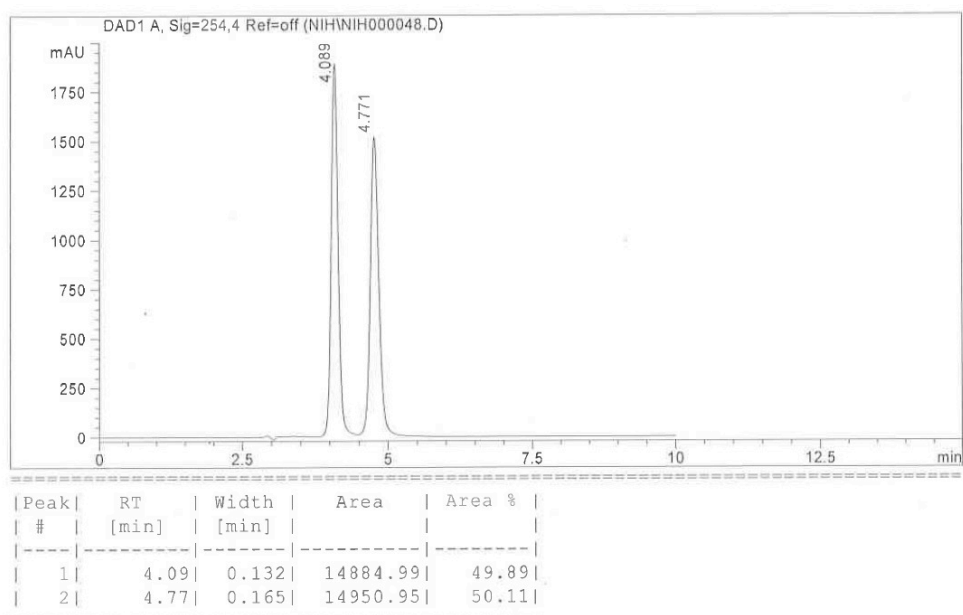
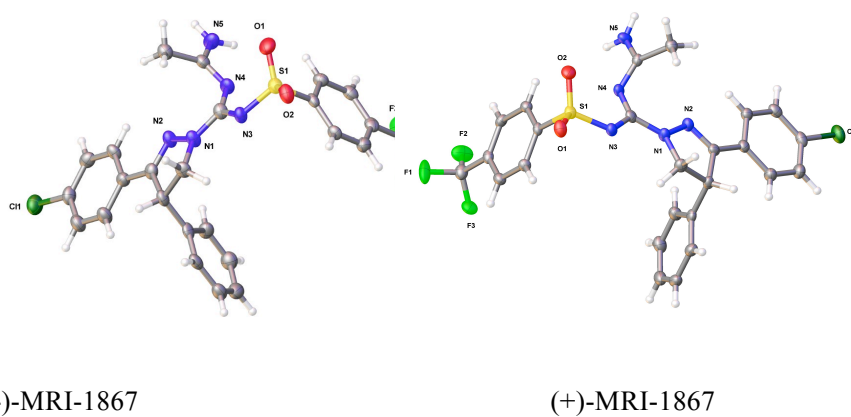
Resat Cinar<sup>1a\*</sup>, Malliga R. Iyer<sup>1a</sup>, Ziyi Liu<sup>1</sup>, Zongxian Cao<sup>2</sup>, Tony Jourdan<sup>1</sup>, Katalin Erdelyi<sup>2</sup>, Grzegorz Godlewski<sup>1</sup>, Gergő Szanda<sup>1</sup>, Jie Liu<sup>1</sup>, Joshua K. Park<sup>1</sup>, Bani Mukhopadhyay<sup>1</sup>, Avi Z. Rosenberg<sup>3</sup>, Jie-Hsan Liow<sup>4</sup>, Robin G. Lorenz<sup>5</sup>, PalPacher<sup>2</sup>, Robert B. Innis<sup>4</sup>, George Kunos<sup>1\*</sup>



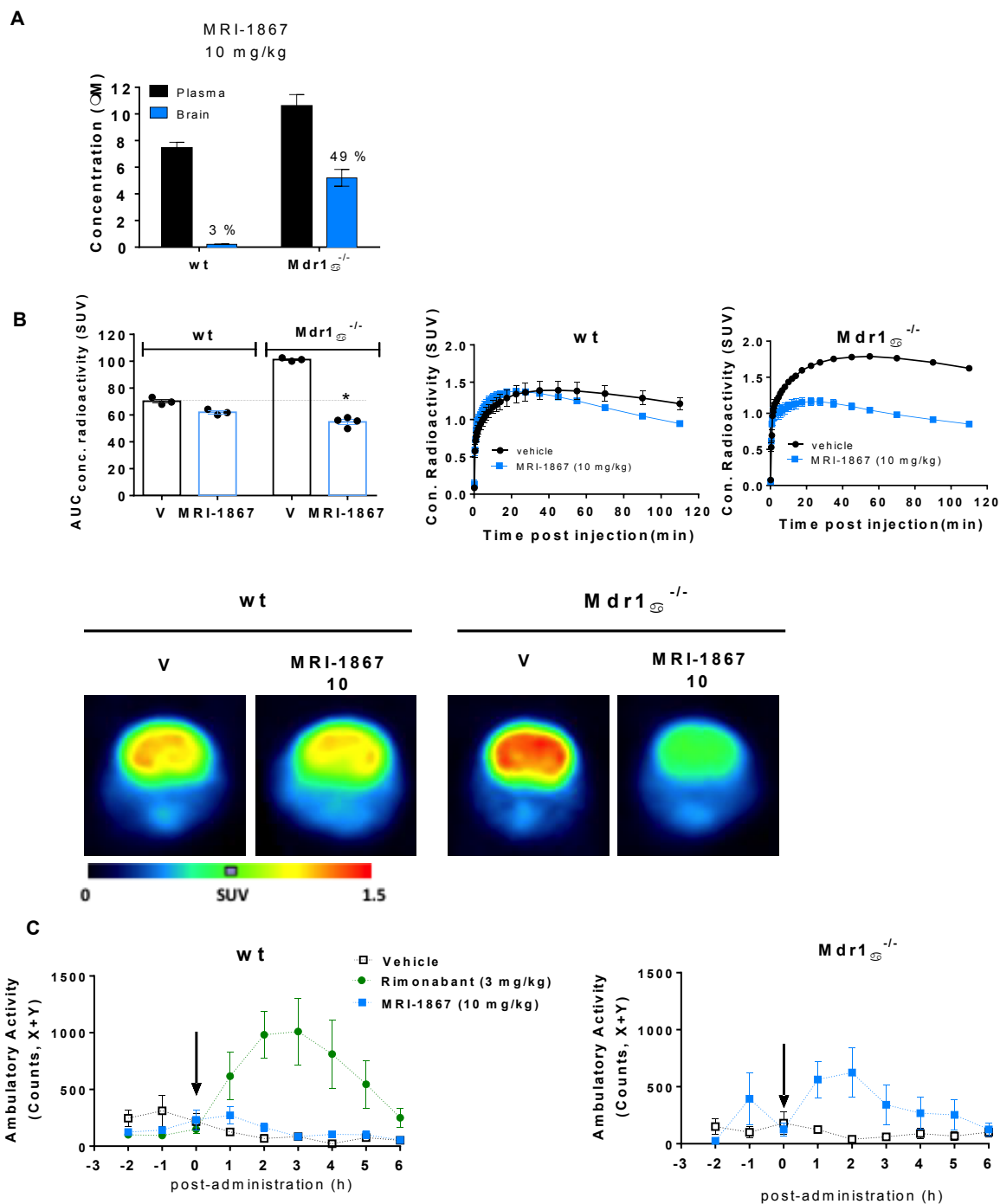
**Supplemental Figure 1.** <sup>1</sup>H NMR spectrum of (-)-MRI-1867 in CDCl<sub>3</sub> (400MHz) using tetramethylsilane as the internal standard.



**Supplemental Figure 2.** <sup>13</sup>C NMR spectrum of (-)-MRI-1867 in DMSO-*d*<sub>6</sub> (101 Mhz)

**A****B**

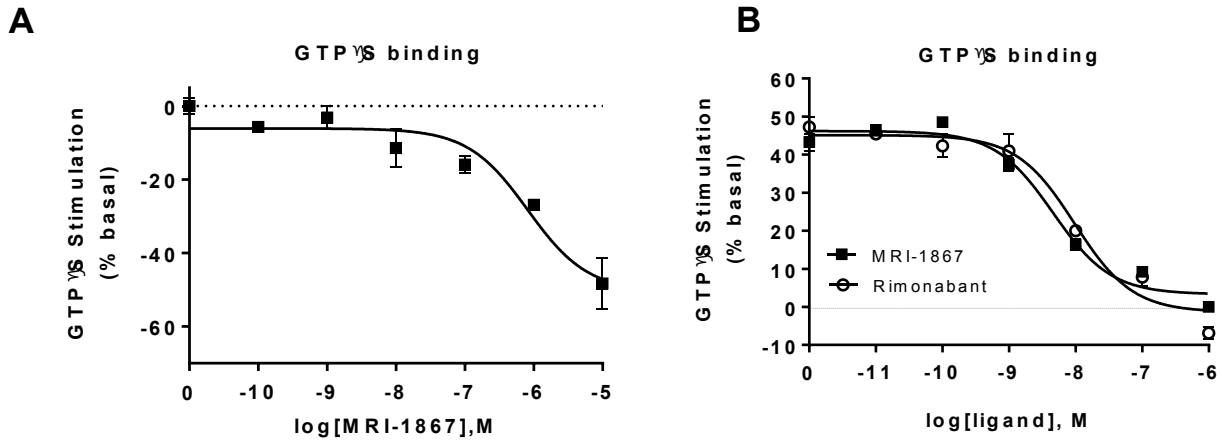
**Supplemental Figure 3.** Analytical Chiral HPLC separation (a) and crystal structure of (-)-MRI-1867 and (+)-MRI-1867 (b).



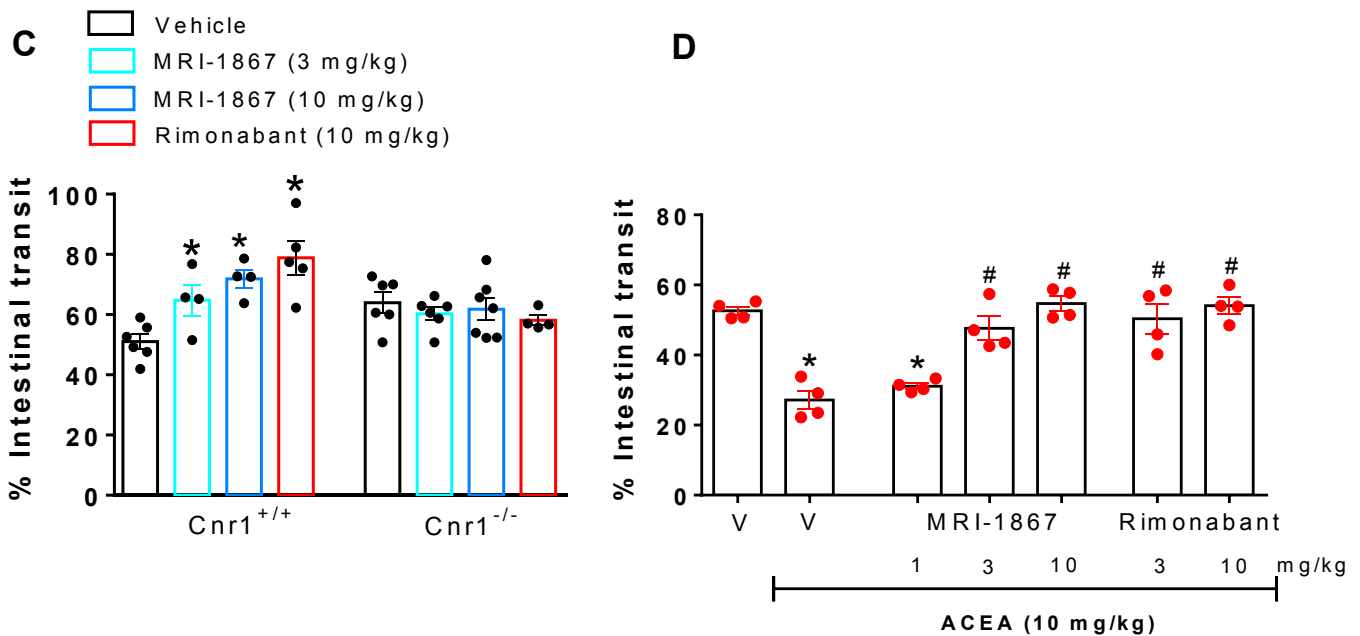
**Supplemental Figure 4. MRI-1867 penetrates the brain and occupies brain CB<sub>1</sub>Rs in MDR1 $\alpha^{-/-}$  mice. (A)**

Brain and plasma concentration of MRI-1867 in wt and MDR1 $\alpha^{-/-}$  mice 1h after acute oral administration of a 10 mg/kg dose; **(B)** MRI-1867 occupancy of brain CB<sub>1</sub>R in MDR1 $\alpha^{-/-}$  mice as indicated by displacement of CB<sub>1</sub>R PET ligand; Data in A and B represent mean  $\pm$  SEM from 3-4 mice/group. **The representative image from a vehicle-treated wild-type mouse is the same as in Fig. 2.** **(C)** MRI-1867, 10 mg/kg, induces hyperambulatory activity in MDR1 $\alpha^{-/-}$  mice, with no such effect in wild-type mice. Data in **C** represent means  $\pm$  SEM from 6 mice/group. Data in **B** was analyzed by t-test. \* indicates significant difference from vehicle group,  $P < 0.05$ .

*in vitro* CB<sub>1</sub>R inverse agonism and antagonism

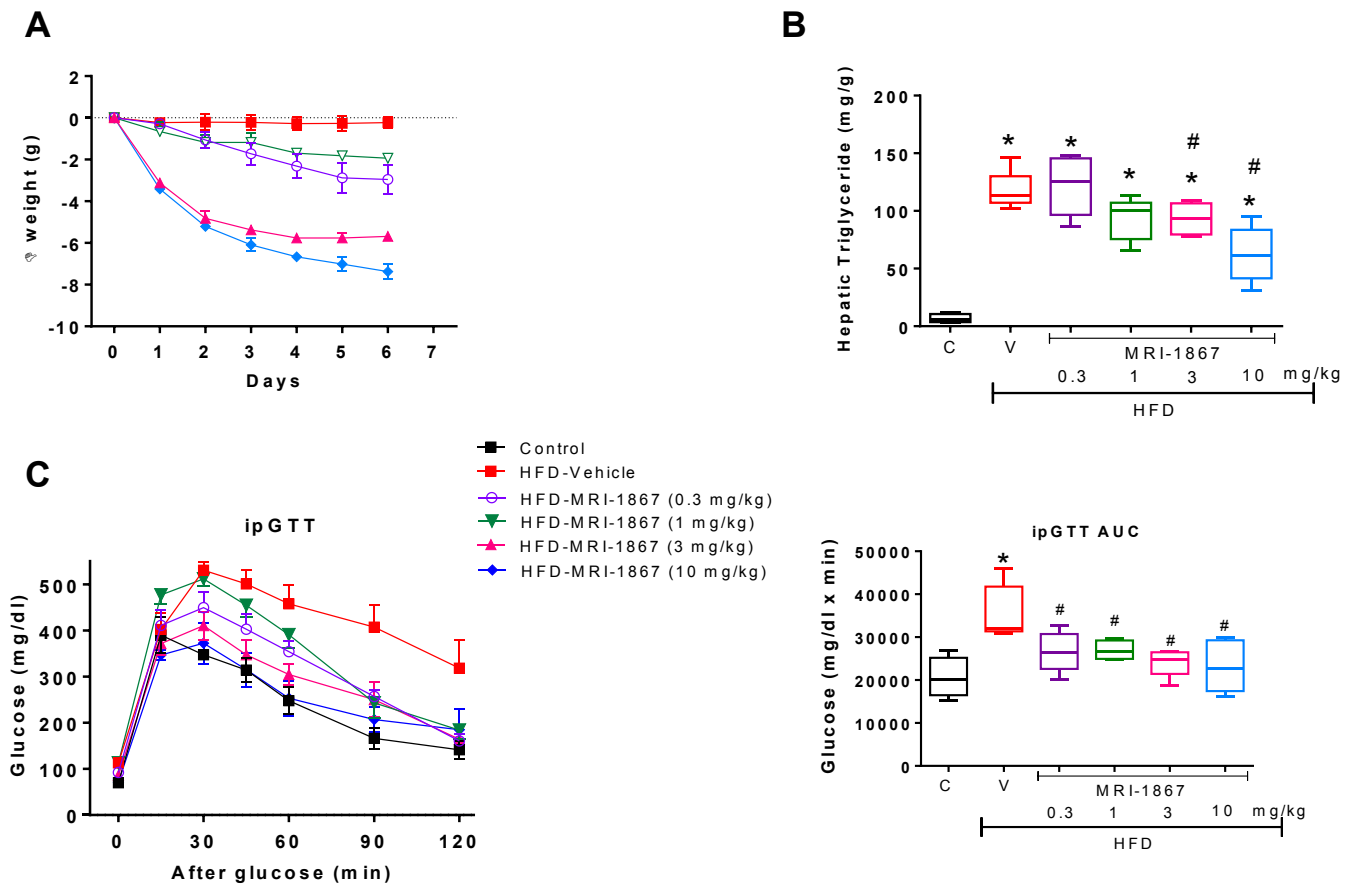


*in vivo* CB<sub>1</sub>R inverse agonism and antagonism



**Supplemental Figure 5. *In vitro* and *in vivo* CB<sub>1</sub>R antagonism and inverse agonism by MRI-1867.** (A) Concentration-dependent effects of MRI-1867 alone or (B) in the presence of 1  $\mu$ M CP55,940 on GTP $\gamma$ S binding, using crude mouse brain membranes. Data in A and B represents means  $\pm$  SEM of three independent experiments performed in triplicate, (C) Effect of MRI-1867 or rimonabant alone on upper GI motility in wt and CB<sub>1</sub>R<sup>-/-</sup> mice. (D) Inhibition by MRI-1867 or rimonabant of the ACEA (CB<sub>1</sub>R agonist)-induced reduction in upper GI motility. Data represent means  $\pm$  SEM from 5-6 mice/group. Data in C and D were analyzed by one-way ANOVA followed by Dunnett's multiple comparisons test. Significant difference from vehicle (\*P<0.05) or ACEA+vehicle group (#P<0.05).





**Supplemental Figure 7. Effects of MRI-1867 on metabolic parameters in DIO mice.** (A) Body weight was measured daily during one week treatment with the indicated daily doses of MRI-1867; (B) Hepatic triglyceride content was determined post-mortem; (C) Glucose tolerance was determined the day after the last daily dose of MRI-1867. Data represent means  $\pm$  SEM from 5-6 mice/group. Data in B and C were analyzed by one-way ANOVA followed by Dunnett's multiple comparisons test. Significant difference from control (\* $P$ <0.05) or vehicle group (# $P$ <0.05).

### Supplemental Table 1.

Effect of MRI-1867 on Caco-2 permeability assay

Compound	Mean A→B $P_{app}$ ( $10^{-6}$ cm S <sup>-1</sup> )	Mean B→A $P_{app}$ ( $10^{-6}$ cm S <sup>-1</sup> )	Efflux ratio $R_E$
MRI-1867	0.67	1.7	2.5
ranitidine	0.53	3.3	6.2
talinolol	0.30	10.1	33.7
warfarin	33.3	10.8	0.3

The assay was performed by Cyprotex (Watertown, MA). Determining the permeability of test agents from apical to basolateral (A→B) or basolateral to apical (B→A), Caco-2 cells were incubated for 2 hours with 10  $\mu$ L transport buffer (1.98 g/L glucose in 10 mM HEPES, 1xHank's balanced Salt solution). Test agents were measured by LC-MS/MS. Efflux ratio ( $R_E$ ) was calculated by ratio of  $P_{app}$  (B→A) /  $P_{app}$  (A→B).  $R_E > 2$  indicates a potential substrate for P-gp or other transporters. Ranitidine, warfarin and talinolol were used as controls for low permeability, high permeability and P-gp efflux, respectively.

**Supplemental Table 2.**

Microsomal stability of MRI-1867

<b>Compound</b>	<b>Test species</b>	<b>NADPH-dependent % remaining (at 60 min)</b>	<b>NADPH-free % remaining (at 60 min)</b>
MRI-1867	mouse	45.9	86.5
	rat	63.1	81.7
	human	57.2	84.7
Verapamil	mouse	0.57	91.2
	rat	0.1	86.8
	human	7.7	86.3
Warfarin	mouse	82	91.3
	rat	88.8	93.1
	human	91.8	97.5

The assay was performed by Cyprotex (Watertown, MA). The drugs were incubated for 60 min in duplicate with liver microsomes from mouse, rat and human (BioReclamation, IVT) at 37°C. The reaction contained microsomal protein (0.3 mg/ml) in 100 mM potassium phosphate, 2 mM NADPH, 3 mM MgCl<sub>2</sub>, pH 7.4. A control reaction was performed for each drug omitting NADPH to detect NADPH-free degradation. Remaining drug levels were determined by LC-MS/MS. Verapamil and Warfarin were used as low and high stability controls, respectively.

### Supplemental Table 3.

Effect of MRI-1867 on AMES mutagenicity test

Test article	Test strain	S9	AMES result (positive/negative)	Highest Concentration tested ( $\mu\text{g/ml}$ )
2-nitrofluorine + 4-nitroquinoline N-oxide	TA98	no	positive	4 + 2
2-nitrofluorine + 4-nitroquinoline N-oxide	TA100	no	positive	4 + 2
aminoanthracene	TA98	yes	positive	5
aminoanthracene	TA100	yes	positive	5
MRI-1867	TA98	no	negative	125
	TA100	no	negative	125
	TA98	yes	negative	125
	TA100	yes	negative	125

The assay was performed by Cyprotex (Watertown, MA). Mutagenic potential of MRI-1867 was assessed in AMES reverse mutation assay in strains TA98 and TA100. The test performed in the presence and absence of S9 metabolic activation. Highest soluble concentration of MRI-1867 at 125  $\mu\text{g/mL}$  was used in the assay.

#### Supplemental Table 4.

Effect of MRI-1867 on the hERG potassium channels

Compound	IC <sub>50</sub> ( $\mu$ M)
MRI-1867	5.106
Cisapride	0.020

FASTPatch hERG assay was performed by ChanTest (Cleveland, OH). The *in vitro* effect of MRI-1867-E1 on the hERG potassium channel current was evaluated at room temperature using the QPatch HT<sup>®</sup> (Sophion Bioscience A/S, Denmark), in human embryonic kidney cells (HEK293).

## Supplemental Table 5.

Off-target interaction profile of MRI-1867 for Safety

Tested receptors	(%) displacement of control specific binding	Target transporters	(%) displacement of control specific binding
A2A	< 50	Norepinephrine transporter	< 50
$\alpha$ 1A adrenergic	< 50	Dopamine transporter	< 50
$\alpha$ 2A adrenergic	< 50	5-HT transporter	< 50
$\beta$ 1 adrenergic	< 50	<b>Target ion channels</b>	
$\beta$ 2 adrenergic	< 50	BZD Benzodiazepine	< 50
CB1 cannabinoid	93	NMDA	< 50
CB2 cannabinoid	< 50	5-HT <sub>3</sub> serotonin	< 50
CCK <sub>1</sub> (CCK <sub>A</sub> ) Cholecystokinin	< 50	Ca <sup>2+</sup> channel (L,dihydropyridine site)	< 50
D <sub>1</sub> dopamine	< 50	hERG	< 50
D <sub>2S</sub> dopamine	< 50	K <sub>v</sub>	< 50
ET <sub>A</sub>	< 50	Na <sup>+</sup> channel (site 2)	< 50
H <sub>1</sub> histamine	< 50	<b>Target Enzymes</b>	<b>(%) inhibition of control</b>
H <sub>2</sub> histamine	< 50	COX <sub>1</sub>	< 50
M <sub>1</sub> muscarinic	< 50	COX <sub>2</sub>	< 50
M <sub>2</sub> muscarinic	< 50	PDE3A	< 50
M <sub>3</sub> muscarinic	< 50	PDE4D <sub>2</sub>	< 50
N neuronal $\alpha$ 4 $\beta$ 2	< 50	Lck kinase	< 50
$\delta$ 2 (DOP) opioid	< 50	acetylcholinesterase	< 50
K (KOP) opioid	61	MAO-A	< 50
$\mu$ (MOP) opioid	< 50		
5-HT <sub>1A</sub> serotonin	< 50		
5-HT <sub>1B</sub> serotonin	< 50		
5-HT <sub>2A</sub> serotonin	< 50		
5-HT <sub>2B</sub> serotonin	< 50		
GR glucocorticoid	< 50		
AR androgen	< 50		
V <sub>1a</sub> arginine vasopressin	< 50		

Safety screen<sup>44</sup> was performed by Eurofins Cerep (Celle l'Evescault, France). 1  $\mu$ M of MRI-1867 was used for the screening experiments. Receptor and transporter binding was calculated as % inhibition of the binding of a radioactively labeled ligand specific for each target. Enzyme inhibition effect was calculated as a% inhibition of control enzyme activity. Inhibition or stimulation >50% are considered to represent significant effects of the test compound.

## Supplemental Table 6.

DiscoverX *gpcr*MAX panel screening of MRI-1867 for off-target GPCR interaction

GPCR	Ago (%)	Antag (%)	GPCR	Ago (%)	Antag (%)	GPCR	Ago (%)	Antag (%)	GPCR	Ago (%)	Antag (%)
ADCYAP1R1	< 20	< 50	CNR1	< 20	<b>100</b>	GLP2R	< 20	< 50	NPY1R	< 20	< 50
ADORA3	< 20	< 50	CNR2	< 20	< 50	GPR1	< 20	< 50	NPY2R	< 20	< 50
ADRA1B	< 20	< 50	CRHR1	< 20	< 50	GPR103	< 20	< 50	NTSR1	< 20	< 50
ADRA2A	< 20	< 50	CRHR2	< 20	< 50	GPR109A	< 20	< 50	OPRD1	< 20	< 50
ADRA2B	< 20	< 50	CRTH2	< 20	< 50	GPR109B	< 20	< 50	OPRK1	< 20	< 50
ADRA2C	< 20	< 50	CX3CR1	< 20	< 50	GPR119	< 20	< 50	OPRL1	< 20	< 50
ADRB1	< 20	< 50	CXCR1	< 20	< 50	GPR120	< 20	< 50	OPRM1	< 20	< 50
ADRB2	< 20	< 50	CXCR2	< 20	< 50	GPR35	< 20	< 50	OXER1	< 20	< 50
AGTR1	< 20	< 50	CXCR3	< 20	< 50	GPR92	< 20	< 50	OXTR	< 20	< 50
AGTRL1	< 20	< 50	CXCR4	< 20	< 50	GRPR	< 20	< 50	P2RY1	< 20	< 50
AVPR1A	< 20	< 50	CXCR5	< 20	< 50	HCRTR1	< 20	< 50	P2RY11	< 20	< 50
AVPR1B	< 20	< 50	CXCR6	< 20	< 50	HCRTR2	< 20	< 50	P2RY12	< 20	< 50
AVPR2	< 20	< 50	CXCR7	< 20	< 50	HRH1	< 20	< 50	P2RY2	< 20	< 50
BDKRB1	< 20	< 50	DRD1	< 20	< 50	HRH2	< 20	< 50	P2RY4	< 20	< 50
BDKRB2	< 20	< 50	DRD2L	< 20	< 50	HRH3	< 20	< 50	P2RY6	< 20	< 50
BRS3	< 20	< 50	DRD2S	< 20	< 50	HRH4	< 20	< 50	PPYR1	< 20	< 50
C3AR1	< 20	< 50	DRD3	< 20	< 50	HTR1A	< 20	< 50	PRLHR	< 20	< 50
C5AR1	< 20	< 50	DRD4	< 20	< 50	HTR1B	< 20	< 50	PROKR1	< 20	< 50
C5L2	< 20	< 50	DRD5	< 20	< 50	HTR1E	< 20	< 50	PROKR2	< 20	< 50
CALCR	< 20	< 50	EBI2	< 20	< 50	HTR1F	< 20	< 50	PTAFR	< 20	< 50
CALCRL-RAMP1	< 20	< 50	EDG1	< 20	< 50	HTR2A	< 20	< 50	PTGER2	< 20	< 50
CALCRL-RAMP2	< 20	< 50	EDG3	< 20	< 50	HTR2C	< 20	< 50	PTGER3	< 20	< 50
CALCRL-RAMP3	< 20	< 50	EDG4	< 20	< 50	HTR5A	< 20	< 50	PTGER4	< 20	< 50
CALCR-RAMP2	< 20	< 50	EDG5	< 20	< 50	KISS1R	< 20	< 50	PTGFR	< 20	< 50
CALCR-RAMP3	< 20	< 50	EDG6	< 20	< 50	LHCGR	< 20	< 50	PTGIR	< 20	< 50
CCKAR	< 20	< 50	EDG7	< 20	< 50	LTB4R	< 20	< 50	PTHR1	< 20	< 50
CCKBR	< 20	< 50	EDG8	< 20	< 50	MC1R	< 20	< 50	PTHR2	< 20	< 50
CCR10	< 20	< 50	EDNRA	< 20	< 50	MC3R	< 20	< 50	RXFP3	< 20	< 50
CCR2	< 20	< 50	EDNRB	< 20	< 50	MC4R	< 20	< 50	SCTR	< 20	< 50
CCR3	< 20	< 50	F2R	< 20	< 50	MC5R	< 20	< 50	SSTR1	< 20	< 50
CCR4	< 20	< 50	F2RL1	< 20	< 50	MCHR1	< 20	< 50	SSTR2	< 20	< 50
CCR5	< 20	< 50	F2RL3	< 20	< 50	MCHR2	< 20	< 50	SSTR3	< 20	< 50
CCR6	< 20	< 50	FFAR1	< 20	< 50	MLNR	< 20	< 50	SSTR5	< 20	< 50
CCR7	< 20	< 50	FPR1	< 20	< 50	MRGPRX1	< 20	< 50	TACR1	< 20	< 50
CCR8	< 20	< 50	FPRL1	< 20	< 50	MRGPRX2	< 20	< 50	TACR2	< 20	< 50
CCR9	< 20	< 50	FSHR	< 20	< 50	MTNR1A	< 20	< 50	TACR3	< 20	< 50
CHRM1	< 20	< 50	GALR1	< 20	< 50	NMBR	< 20	< 50	TBXA2R	< 20	< 50
CHRM2	< 20	< 50	GALR2	< 20	< 50	NMU1R	< 20	< 50	TRHR	< 20	< 50
CHRM3	< 20	< 50	GCGR	< 20	< 50	NPBWR1	< 20	< 50	TSHR(L)	< 20	< 50
CHRM4	< 20	< 50	GHSR	< 20	< 50	NPBWR2	< 20	< 50	UTR2	< 20	< 50
CHRM5	< 20	< 50	GIPR	< 20	< 50	NPPFR1	< 20	< 50	VIPR1	< 20	< 50
CMKLR1	< 20	< 50	GLP1R	< 20	< 50	NPSR1B	< 20	< 50	VIPR2	< 20	< 50

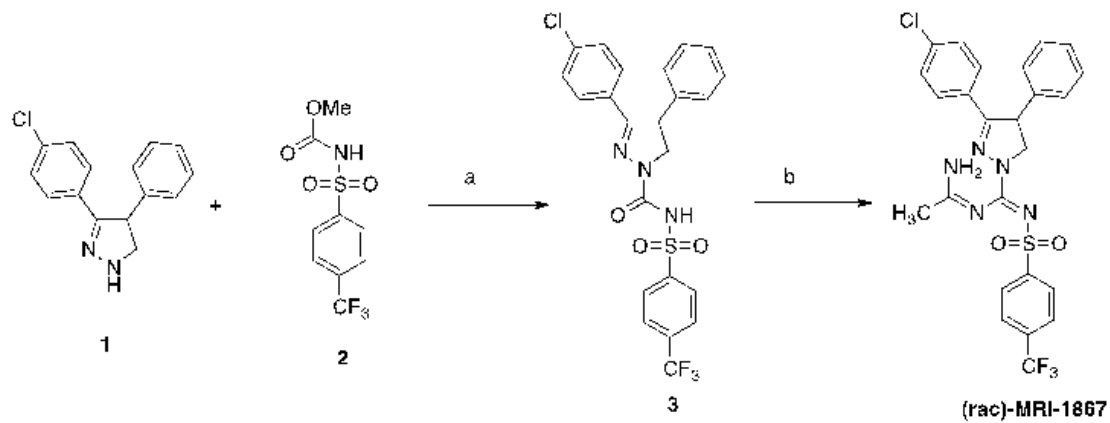
*gpcr*MAX panel screening assay was performed by DiscoverX (Fremont, CA). MRI-1867 (1  $\mu$ M) was screened against both agonist and antagonist mode. Over 20% stimulation or 50% inhibition considered as significant effect for agonism or antagonism, respectively.

## SUPPLEMENTAL METHODS

*Methods used in the chemical synthesis and analysis of MRI-1867.* Reagents available commercially were purchased and used as is. Melting points were determined on a Buchi B-545 instrument and are uncorrected. Proton and carbon nuclear magnetic resonance ( $^1\text{H}$  and  $^{13}\text{C}$  NMR) spectra were recorded on a Varian 400 spectrometer in  $\text{CDCl}_3$  or  $\text{DMSO-d}_6$  (unless otherwise noted) with the values given in ppm (TMS as internal standard) and  $J$  (Hz) assignments of  $^1\text{H}$  resonance coupling. Mass spectra (HRMS) were recorded on a VG 7070E spectrometer or a JEOL SX102a mass spectrometer. Thin layer chromatography (TLC) analyses were carried out on Analtech silica gel GHLF 0.25 mm plates using various gradients of  $\text{CHCl}_3/\text{MeOH}$  containing 1%  $\text{NH}_4\text{OH}$  or gradients of  $\text{EtOAc}:n\text{-hexane}$ . Visualization was accomplished under UV light or by staining in an iodine chamber. Flash column chromatography was performed on Teledyne ISCO Combiflash system with PuriOn mass detector. All derivatives synthesized and tested had  $> 95\%$  purity. LC/MS detection was carried out on Agilent 1200 using Luna C18 3  $\mu\text{m}$  (3 x 75 mm). The mobile phase was 4% to 100% acetonitrile (0.05% TFA) standard gradient. The LC-MS chromatogram showed the correct molecular ( $\text{MH}^+$ ) ion as well as a single peak by both UV (254 nm). Micro-Analysis, Inc., Wilmington, DE, performed elemental analyses, and the results were within 0.4% of the theoretical values. X-ray results were obtained utilizing the X-ray facility at University of California San Diego. Gram-scale chiral separation of (*rac*)-MRI-1867 was carried out at Regis Technologies Inc.

*Synthesis, purification and isolation of compound MRI-1867.*

Scheme 1



Reagents and conditions: (a) Toluene, reflux; (b) i. PCl<sub>5</sub>, chlorobenzene, reflux; ii. Acetamidine•HCl, Et<sub>3</sub>N, MeOH: CH<sub>2</sub>Cl<sub>2</sub>, 78°C

*3-(4-chlorophenyl)-4-phenyl-4,5-dihydro-1H-pyrazole (1)*. Compound **1** was synthesized as described (1, 2).

*Methyl (4-(trifluoromethyl)phenyl)sulfonylcarbamate (2)*. A stirred solution of 4-trifluoromethyl sulfonamide (6.48 g, 28.8 mmol) and Et<sub>3</sub>N (12 mL, 86.4 mmol) in acetonitrile (100 ml) was treated with methyl chloroformate (3.34 mL, 43.2 mmol) at 0°C. The reaction was warmed to room temperature over 6 h and the solvent evaporated in vacuo. The residue was dissolved in ethyl acetate and aqueous NaHCO<sub>3</sub> was added. The water layer was extracted and acidified with concentrated HCl in ice to give an oily emulsion, which turned into a white precipitate upon standing. The fluffy precipitate was filtered, washed with water and dried to give compound **2** (5.2 g, 64%). Mp: 85-87 C; <sup>1</sup>H-NMR (400 MHz, CDCl<sub>3</sub>): δ 8.19 (d, *J* = 8.3 Hz, 2H), 7.82 (d, *J* = 8.4 Hz, 2H), 3.71 (s, 3H), 2.18 (s, NH); <sup>13</sup>C-NMR (101 MHz, CDCl<sub>3</sub>) δ 150.9, 141.8, 136.2-135.2(q), 129.10, 126.4-126.3 (q), 124.5, 121.8, 53.9; LRMS (C<sub>9</sub>H<sub>10</sub>F<sub>3</sub>NO<sub>4</sub>S) [M+Na]<sup>+</sup>: C<sub>9</sub>H<sub>10</sub>F<sub>3</sub>NO<sub>4</sub>S 306.0

*3-(4-Chlorophenyl)-4-phenyl-N-((4-(trifluoromethyl)phenyl)sulfonyl)-4,5-dihydro-1H-pyrazole-1-carboxamide (3)*. To a solution of **2** (1 g, 3.53 mmol) in toluene, compound **1** (994 mg, 3.88 mmol) was added and the mixture was refluxed for 5 h. The solution was cooled to room temperature and compound **3** crystallized out of the solution. The crystals were collected and washed with cold toluene to yield pure **3** (1.1 g, 61%). Mp: 198-200 C;

<sup>1</sup>H-NMR (400 MHz, CDCl<sub>3</sub>) δ 8.89 (s, 1H), 8.30 (d, *J* = 8.1 Hz, 2H), 8.30 (d, *J* = 8.1 Hz, 2H), 7.81 (d, *J* = 8.2 Hz, 2H), 7.53 (d, *J* = 8.4 Hz, 2H), 7.25 (d, *J* = 8.3 Hz, 5H), 7.10 (d, *J* = 7.0 Hz, 2H), 4.71 (dd, *J* = 11.6, 5.4 Hz, 1H), 4.31 (t, *J* = 11.6 Hz, 1H), 3.89 (dd, *J* = 11.5, 5.5 Hz, 1H). <sup>13</sup>C-NMR (101 MHz, CDCl<sub>3</sub>): δ 156.7, 147.7, 142.6, 139.1, 136.8, 135.8-134.9 9 (q), 129.6, 129.2, 129.1, 128.8, 128.3, 128.1, 127.3, 126.2-126.1 (q), 124.6, 121.9, 54.1, 51.6; LRMS (C<sub>23</sub>H<sub>18</sub>ClF<sub>3</sub>N<sub>3</sub>O<sub>3</sub>S) [M+H]<sup>+</sup>: 508.1.

*N-(1-aminoethylidene)-3-(4-chlorophenyl)-4-phenyl-N'-((4-(trifluoromethyl)phenyl) sulfonyl)-4,5-dihydro-1H-pyrazole-1-carboximidamide (rac)-MRI-1867*). Compound **3** (1 g, 1.96 mmol)

and  $\text{PCl}_5$  (489 mg, 2.35 mmol) were taken up in chlorobenzene (10 mL) and refluxed for 1 h. After thorough evaporation of the solvent, the formed imidoyl chloride (structure not shown) was dissolved in  $\text{CH}_2\text{Cl}_2$  and cooled to  $-78^\circ\text{C}$ . Acetamidine•HCl (278 mg, 2.94 mmol) premixed with  $\text{Et}_3\text{N}$  (2 mL-) in MeOH:  $\text{CH}_2\text{Cl}_2$  (1:1) (20 ml) was added drop-wise. The reaction was slowly allowed to warm up to room temperature overnight. The reaction mixture was washed with water and extracted with  $\text{CH}_2\text{Cl}_2$  and the solvent evaporated. The residue was subjected to flash chromatography and purified using 60% EtOAc in hexanes. The pale yellow solid was triturated with Isopropyl alcohol to give a white powder (320 mg, 30% yield).

Mp: 228-230  $^\circ\text{C}$ ;  $^1\text{H-NMR}$  (rac)-MRI1867 (400 MHz,  $\text{CDCl}_3$ )  $\delta$  8.05 (d,  $J = 7.9$  Hz, 2H), 7.68 (d,  $J = 8.1$  Hz, 2H), 7.50 (d,  $J = 8.5$  Hz, 2H), 7.29 (d,  $J = 7.2$  Hz, 3H), 7.21 (d,  $J = 8.6$  Hz, 2H), 7.08 (d,  $J = 6.9$  Hz, 2H), 5.21 (s, 2H), 4.74-4.70 (m, 1H), 4.50 (t,  $J = 11.9$  Hz, 1H), 4.12-4.08 (m, 1H), 2.09 (s, 3H);  $^{13}\text{C-NMR}$  (101 MHz,  $\text{DMSO-d}_6$ )  $\delta$  160.5, 158.4, 158.3, 147.6, 140.2, 134.8, 131.0, 130.6, 129.2, 129.0, 128.8, 128.6, 127.9, 127.5, 127.3, 125.3, 125.3, 125.1, 122.4, 56.3, 49.6, 20.2; HRMS ( $\text{C}_{25}\text{H}_{22}\text{ClF}_3\text{N}_5\text{O}_2\text{S}$ )  $[\text{M}+\text{H}]^+$ : calc 548.1129 found: 548.1132.

*(4S)-(-)-N-(1-aminoethylidene)-3-(4-chlorophenyl)-4-phenyl-N'-((4-(trifluoromethyl)phenyl)sulfonyl)-4,5-dihydro-1H-pyrazole-1-carboximidamide ((-)-MRI-1867*. Chiral preparative HPLC separation on racemic compound (100 mg) using a (R,R)-Whelk-O1 as the chiral stationary phase (25 cm x 21mm) yielded (-)-MRI-1867 (38 mg) and (+)-MRI-1867 (45 mg), respectively. The mobile phase was 100% ethanol.

$[\alpha]_D^{25} = -16.2$ ,  $c = 0.185$ ,  $\text{CHCl}_3$ ; Mp 144-146  $^\circ\text{C}$ ;  $^1\text{H-NMR}$  (-)-MRI-1867 (400 MHz,  $\text{CDCl}_3$ ):  $\delta$  8.05 (d,  $J = 8.0$  Hz, 2H), 7.68 (d,  $J = 8.2$  Hz, 2H), 7.49 (d,  $J = 8.6$  Hz, 2H), 7.29 (q,  $J = 6.2$  Hz, 3H), 7.21 (d,  $J = 8.6$  Hz, 2H), 7.08 (d,  $J = 6.9$  Hz, 2H), 5.25 (s, 2H), 4.72 (dd,  $J = 11.4$ , 5.0 Hz, 1H), 4.50 (t,  $J = 12.0$  Hz, 1H), 4.10 (dd,  $J = 12.3$ , 4.6 Hz, 1H), 2.08 (s, 3H);  $^{13}\text{C-NMR}$  (101 MHz,  $\text{CDCl}_3$ ):  $\delta$  160.4, 159.1, 158.5, 146.7, 139.3, 136.6, 133.3-133.0 (q), 129.7, 129.0, 128.8, 128.6, 128.1, 127.8, 127.2, 125.4, 125.1, 122.3, 56.6, 51.1, 20.8.  $^{13}\text{C-NMR}$  (101 MHz,  $\text{DMSO-d}_6$ ):  $\delta$  160.5, 158.4, 158.3, 147.6, 140.2, 134.8, 131.0, 130.7, 129.2, 129.0, 128.8, 128.6, 127.9, 127.5, 127.3, 125.4, 125.3, 125.1, 122.4, 56.3, 49.6, 20.2. HRMS ( $\text{C}_{25}\text{H}_{22}\text{ClF}_3\text{N}_5\text{O}_2\text{S}$ )  $[\text{M}+\text{H}]^+$ : calc 548.1129 found: 548.1132. Anal. calc'd for  $\text{C}_{25}\text{H}_{21}\text{ClF}_3\text{N}_5\text{O}_2\text{S}$ : C, 54.80; H, 3.86; N, 12.78; found: C, 54.66; H, 3.63; N, 12.66.

(4*R*)-(+)-*N*-(1-aminoethylidene)-3-(4-chlorophenyl)-4-phenyl-*N'*-((4-(trifluoromethyl)phenyl)sulfonyl)-4,5-dihydro-1*H*-pyrazole-1-carboximidamide ((+)-MRI-1867)

[ $\alpha$ ]<sub>D</sub> = +16.2 c = 0.185, CHCl<sub>3</sub>; Mp 144-146 °C; <sup>1</sup>H-NMR (400 MHz, CDCl<sub>3</sub>): δ 8.05 (d, *J* = 8.0 Hz, 2H), 7.68 (d, *J* = 8.2 Hz, 2H), 7.49 (d, *J* = 8.6 Hz, 2H), 7.29 (d, *J* = 7.3 Hz, 3H), 7.21 (d, *J* = 8.6 Hz, 2H), 7.08 (d, *J* = 6.9 Hz, 2H), 5.26 (s, 2H), 4.72 (dd, *J* = 11.4, 5.1 Hz, 1H), 4.50 (t, *J* = 12.0 Hz, 1H), 4.10 (dd, *J* = 12.4, 4.7 Hz, 1H), 2.08 (s, 3H); <sup>13</sup>C-NMR (101 MHz, DMSO-*d*<sub>6</sub>) δ 160.5, 158.4, 158.3, 147.6, 140.2, 134.8, 131.0, 130.6, 129.2, 129.0, 128.8, 128.6, 127.9, 127.5, 127.3, 125.4, 125.3, 125.1, 122.4, 56.3, 49.6, 20.2; HRMS (C<sub>25</sub>H<sub>22</sub>ClF<sub>3</sub>N<sub>5</sub>O<sub>2</sub>S) [M+H]<sup>+</sup>: calc'd: 548.1129 found: 548.1132.

#### *X-Ray Diffraction.*

**1.** (-)-MRI-1867. The absolute stereochemical configuration of (-)-MRI-1867 was determined by X-Ray diffraction (Supplemental Fig. 3b). The compound was dissolved in IPA:Water (9:1) and the solution was kept overnight for three days at room temperature. The single crystal X-ray diffraction studies were carried out on a Bruker Kappa APEX-II CCD diffractometer equipped with Mo K<sub>α</sub> radiation (*λ* = 0.71073 Å). A 0.315 x 0.033 x 0.021 mm piece of a colorless needle was mounted on a Cryoloop with Paratone oil. Data were collected in a nitrogen gas stream at 100(2) K using *f* and *v* scans. Crystal-to-detector distance was 40 mm and exposure time was 20 seconds per frame using a scan width of 1.0°. Data collection was 99.9% complete to 25.00° in *q*. A total of 46788 reflections were collected covering the indices, -23 ≤ *h* ≤ 23, -8 ≤ *k* ≤ 8, -26 ≤ *l* ≤ 26. 10167 reflections were found to be symmetry independent, with a *R*<sub>int</sub> of 0.0586. Indexing and unit cell refinement indicated a primitive, monoclinic lattice. The space group was found to be *P*2<sub>1</sub>. The data were integrated using the Bruker SAINT software program and scaled using the SADABS software program. Solution by direct methods (SHELXT) produced a complete phasing model consistent with the proposed structure. All non-hydrogen atoms were refined anisotropically by full-matrix least-squares (SHELXL-2014). All hydrogen atoms were placed using a riding model. Their positions were constrained relative to their parent atom using the appropriate HFIX command in SHELXL-2014. Atomic coordinates for (-)-MRI1867 have been deposited with the Cambridge Crystallographic Data Centre (deposition number: 1410998). Copies of the data can be obtained, free of charge, on application to CCDC, 12 Union Road, Cambridge, CB2 1EZ, UK [fax: +44(0)-1223-336033 or e-mail: [deposit@ccdc.cam.ac.uk](mailto:deposit@ccdc.cam.ac.uk)]

2. (+)-MRI-1867. The absolute stereochemical configuration of (+)-MRI-1867 was determined by X-Ray diffraction (Supplemental Figure 3B). The compound was dissolved in IPA:Water (9:1) and the solution was kept overnight for three days at room temperature. The single crystal X-ray diffraction studies were carried out on a Bruker Kappa APEX-II CCD diffractometer equipped with Mo  $K_{\alpha}$  radiation ( $\lambda = 0.71073 \text{ \AA}$ ). A 0.135 x 0.013 x 0.011 mm piece of a colorless needle was mounted on a Cryoloop with Paratone oil. Data were collected in a nitrogen gas stream at 100(2) K using  $\omega$  and  $\nu$  scans. Crystal-to-detector distance was 40 mm and exposure time was 10 seconds per frame using a scan width of  $1.0^{\circ}$ . Data collection was 100% complete to  $25.00^{\circ}$  in  $q$ . A total of 11265 reflections were collected covering the indices,  $-24 \leq h \leq 24$ ,  $-8 \leq k \leq 8$ ,  $-27 \leq l \leq 27$ . 11265 reflections were found to be symmetry independent, with a  $R_{\text{int}}$  of 0.0458. Indexing and unit cell refinement indicated a primitive, monoclinic lattice. The space group was found to be  $P2_1$ . The data were integrated using the Bruker SAINT software program and scaled using the SADABS software program. Solution by direct methods (SHELXT) produced a complete phasing model consistent with the proposed structure. All non-hydrogen atoms were refined anisotropically by full-matrix least-squares (SHELXL-2014). All carbon bonded hydrogen atoms were placed using a riding model. Their positions were constrained relative to their parent atom using the appropriate HFIX command in SHELXL-2014. All other hydrogen atoms (H-bonding) were located in the difference map. Their relative positions were restrained using DFIX commands and their thermals freely refined. Atomic coordinates for (+)-MRI1867 have been deposited with the Cambridge Crystallographic Data Centre (deposition number: 1410998). Copies of the data can be obtained, free of charge, on application to CCDC, 12 Union Road, Cambridge, CB2 1EZ, UK [fax: +44(0)-1223-336033 or e-mail: [deposit@ccdc.cam.ac.uk](mailto:deposit@ccdc.cam.ac.uk)]

1. Grosscurt, A.C., van Hes, R., and Wellinga, K. 1979. 1-Phenylcarbamoyl-2-pyrazolines, a new class of insecticides. 3. Synthesis and insecticidal properties of 3,4-diphenyl-1-phenylcarbamoyl-2-pyrazolines. *J. Agric. Food. Chem.* 27:406-409.
2. Lange, J.H., Coolen, H.K., van Stuijvenberg, H.H., Dijkman, J.A., Herremans, A.H., Ronken, E., Keizer, H.G., Tipker, K., McCreary, A.C., Veerman, W., et al. 2004. Synthesis, biological properties, and molecular modeling investigations of novel 3,4-diarylpyrazolines as potent and selective CB(1) cannabinoid receptor antagonists. *J Med Chem* 47:627-643.